

Pair correlations and magnetic susceptibility of small Al-grains

N.K. Kuzmenko¹⁾, V.M. Mikhajlov²⁾
and S.Frauendorf³⁾

¹⁾*V.G. Khlopin Radium Institute, 194021, St.-Petersburg, Russia*

²⁾*Institute of Physics St.-Petersburg State University 198904, Russia*

³⁾*IKHP, Forschungszentrum Rossendorf e.V., PF 510119, 01314 Dresden, Germany*

Abstract

Pair correlations and the magnetic susceptibility of electrons in a spherical cavity are studied both for grand canonical and the canonical ensemble. The coupling constant of the *BCS* Hamiltonian is adjusted to experimental values of the gap parameter. The gap parameter is found to increase for small grains as a consequence of the pronounced shell structure in the spectrum of the spherical cavity. The sharp phase transition at T_c is smeared out for the canonical ensemble. The strong paramagnetic susceptibility of the normal electrons in the cavity is reduced by the superconductivity, but it remains positive.

1 Introduction

Whereas many properties of superconducting bulk metals at low temperatures have been well studied, the influence of size effects on the same properties of small metal grains or clusters is still a problem of a current interest. The minimal size of grains in which the phenomenon of superconductivity can be observed has not been established by now. It has been known for about three decades that metal grains on the nanometer-scale display superconductivity [1].

The focus of the paper are the electronic finite size effects in the grains, which reveal themselves not only in the discreteness of the energies of the electron states but also in their shell structure. This means, that the level density strongly fluctuates as function of the energy. In regions with high level density the pair correlations are enhanced. This kind of enhancement has been demonstrated for electrons confined to a slab [2] and to a cube [3]. In this paper we are going to investigate the same effect as well as the magnetic response of small grains by means of yet another very simple model. It is assumed that the electrons are confined inside a sphere or hemisphere with a perfect surface and that only the electrons on the highly degenerated Fermi level take part in the pair correlations. The spherical model has a very pronounced shell structure. In this respect it contrasts the extended Landau - Ginzburg model for grains [4], which does not take into account any shell structure. Comparing these two extremes will provide insight into the properties of real grains with electronic shell structure. Though the model is a very strong idealization of realistic grains it has the advantage that the exact solutions of the many body problem with finite particle number are known. This permits to exactly calculate finite size effects due the conservation of the electron number as well as the enhancement of the magnetic response in a finite system. It also allows to judge the typical approximations (mean field approximation, grand canonical ensemble) one has to resort to in more realistic models of the electron system of the grain. In particular, it will be demonstrated that the strong shell structure of the (hemi) sphere generates a dramatic enhancement of the pair correlations with decreasing size, resulting in a growth of the transition temperature.

The experimental transition temperatures $T_c(N)$ for grains with N delocalized electrons turn out to be larger than or equal to the bulk value. For Al, a weak-coupling superconducting metal, the measured ratio $f = T_c(N)/T_c(bulk)$ grows considerably with decreasing N : $f \approx 1.5$ for $N \sim 10^5$ and $f \approx 3$ for $N \sim 10^3$ [5, 6, 7]. Grains of intermediate-coupling metals show a more moderate growth of $T_c(N)$: $f \approx 1.2$ for In grains with $N \sim 10^5$ [5], $f \approx 1.1$ for Sn grains with $N \sim 10^6$ [8]. For strong-coupling Pb the transition temperature $T_c(N)$ is about equal to the bulk value down to grains with $N \sim 10^3$ [5]. Recently, Black, Ralf and Tinkham [9, 10] provided additional evidence. By tunneling experiments on grains of $R \sim (5-10)$ nm, the pairing gap Δ has been measured to be as large as ~ 2 times the bulk value.

The increase of the transition temperature and the pairing gap has been attributed to an increase of the coupling constant λ with decreasing size of the grains. Various theoretical

models have been suggested for explanation of such an increase [5, 11, 12, 13, 14, 15, 16, 17]. In this work we do not investigate the possible mechanisms behind such a change of the coupling constant. Rather, we choose a phenomenological approach, introducing an explicit dependence of the effective interaction strength λ on the electron number N . We are going to demonstrate that in studying the N - dependence of the coupling constant the shell structure has to be taken into account.

The BCS theory of our model is exposed in sections 2 and 3. We limit ourselves to Al grains with $10^3 < N < 10^5$, for which the best experimental data on Δ are available. In section 4., these are used to determine $G(N)$ by comparing the empirical and calculated values of $T_c(N)$.

It is known [8, 18] that the specific heat $C(T)$ of superconducting metallic grains does not show the singularity at T_c seen in bulk metals. For grains, the function $C(T)$ has a maximum at T_0 that is smaller than T_c for bulk metals. With decreasing grain size this maximum shifts to smaller temperature and the width of the peak becomes wider. The question arises, how to define a transition temperature T_c from the non-singular function $C(T)$. Calculations in the grand canonical BCS approximation cannot reproduce the observed T -dependence of C . Therefore, in section 5 the influence of the superconductivity on $C(T)$ is studied within the canonical ensemble. The results suggest a definition of T_c , which coincides with the one in *BCS* theory as well as with previous definitions, introduced for interpreting the measurements of $C(T)$ [8, 18] and electromagnetic properties [17, 18] in grains.

Superconducting bulk metals show the Meissner effect. The diamagnetic susceptibility takes its maximum, compensating completely external magnetic field inside the metal. For grains with sizes comparable or smaller than the coherence and penetration lengths an incomplete compensation is expected, which will be investigated in section 6. The issue is complicated by the fact, that in normal (non-superconducting) grains the susceptibility at low temperatures strongly deviates from its bulk values. Both para- and diamagnetic enhancements appear a certain electron numbers, reflecting the electronic shell structure of the grain. This has recently been studied in [19, 20, 21], where the references to further work can be found. Hence, an intricate interplay between the paramagnetism due to the shell structure and the diamagnetism due to the superconductivity is expected for superconducting grains, which will also be studied in section 6.

2 The spherical cavity model in *BCS* approximation

We consider N electrons in a cavity of radius $R = r_0 N^{1/3}$, i. e. we employ the spherically symmetric rectangular well with infinite walls as a simplified model of the mean field that confines the delocalized electrons of the grain. The energies e_t are given by the roots of the Bessel functions.

Thus, we describe the system of N electrons by means of the effective electron Hamil-

tonian

$$H - \mu N = \sum (e_t - \mu) a_t^\dagger a_t - G(N) \sum a_t^\dagger a_{\bar{t}}^\dagger a_{\bar{s}} a_s. \quad (1)$$

The interaction strength G is treated as a parameter that is fixed by comparison with the experimental pair gaps $\Delta(N)$ measured for different grain sizes. The pairing interaction in (1) acts only among electron levels inside the interval $|e_t - \mu| < \hbar\omega_D$, where the Debye frequency is taken to be the same as in the bulk.

The treatment of the Hamiltonian (1) in *BCS* mean field approximation is a standard problem in nuclear physics. For example it is exposed in the textbook [22]. We have solved the problem numerically. If a grain contains 10^3 or more delocalized electrons the single-particle spectrum poses a high degeneracy in the vicinity of the Fermi level (F). The average orbital momentum l is of order $N^{1/3}$. Each level can be occupied by about $4 \cdot N^{1/3}$ electrons. The number of these degenerated levels inside the Debye interval $2\hbar\omega_D$ varies from 1 ($N \sim 10^3$) to 5 ($N \sim 10^5$). However, as demonstrated in fig. 1, practically it is sufficient to take into account the Fermi level alone because for particle numbers ($10^3 < N < 10^5$) the distance to next levels is always much larger than the pairing gap Δ , found by means of the full *BCS* equations. The isolation the Fermi level and its high degeneracy are the conditions to apply the *single shell model* [22] for pairing. This approximation takes into account only the pair interaction among the electrons in the partially filled Fermi level. In the grand canonical *BCS* approximation, the single shell model was used in [23] for a half filled shell. We consider the case of arbitrary numbers of particles in the shell and, in sections 5 and 6, the canonical ensemble of the exact many body states.

In the single shell approximation, which we are going to study, the spherical cavity is equivalent with a hemisphere. This is seen as follows. The wave functions in the spherical cavity have good orbital angular momentum l . All wave functions with odd l are equal to zero in the the plane $z = 0$. Thus, they fulfill also the boundary condition for the hemisphere and are (with the appropriate choice of the normalization) the wave function of this type of cavity. None of the conclusions drawn below depends on l being odd or even. Thus, they are valid for the hemisphere as well. Clusters on surfaces, the superconductivity of which is studied experimentally, have the shape of somewhat flattened hemispheres.

The single shell approximation leads to considerable simplifications because there are no summations over single particle states in the *BCS* equations and many quantities become analytical expressions of the temperature and the filling parameter

$$n = \frac{N_{sh}}{2M}, \quad M = 2l + 1, \quad (2)$$

where N_{sh} is the actual and $2(2l + 1)$ the maximal number of electrons on the Fermi level, which has $M = 2l + 1$ magnetic substates and 2 orientations of the spin. There is only one quasiparticle energy

$$E = \sqrt{(e - \mu)^2 + \Delta^2}, \quad (3)$$

which is independent of n at zero temperature,

$$E(0) = \frac{GM}{2}. \quad (4)$$

At finite temperature the quasiparticle energy is obtained as the solution of the implicit equation

$$E = E(0) \tanh\left\{\frac{E}{2T}\right\}. \quad (5)$$

Independent of temperature, the difference between the Fermi level and chemical potential is given by

$$e - \mu = E(0)(1 - 2n) \quad (6)$$

The pairing gap Δ has a maximum in the middle of the shell ($n = 1/2$). It is given by

$$\Delta = \sqrt{E^2 - (e - \mu)^2}. \quad (7)$$

Its zero temperature value is

$$\Delta(0) = 2E(0)\sqrt{n(1-n)}. \quad (8)$$

As displayed in Fig. 2, a finite temperature T decreases Δ but its behavior as a function of n is similar to that at $T = 0$. Our calculations of Δ with all single particle levels inside the Debye interval give results practically indistinguishable from those in Fig. 2. This demonstrates the applicability of the single shell approximation for the considered values of N and T .

The transition temperature T_c is defined as the temperature where Δ disappears. It is obtained from Eq.(5), substituting the value of the expression (3) at $\Delta = 0$ for E , i. e.

$$|e - \mu| = E(0) \frac{\exp\{|e - \mu|/T_c\} - 1}{\exp\{|e - \mu|/T_c\} + 1}. \quad (9)$$

Taking into account the expression (6) for the chemical potential the transition temperature is given by

$$T_c(n) = 2E(0)\xi^{-1}(n), \quad (10)$$

$$\xi(n) = 2x^{-1} \ln \frac{1+x}{1-x}, \quad x = |1 - 2n|, \quad 0 < x < 1.$$

As shown in Fig.3, T_c is symmetric with respect to exchanging $n \rightarrow 1 - n$. In the middle of the shell ($n = 1/2$, $x = 0$) the limit $x \rightarrow 0$ in Eq.(10) gives the known result [22] $\xi(n = 1/2) = 4$, which coincides with the value obtained Parameter [3] for a cubic cavity.

In the *BCS* theory of bulk metals there is the universal relation between T_c and $2\Delta(0)$ which is the energy of the lowest two-quasiparticle excitation,

$$\frac{2\Delta(0)}{T_c} = \frac{2E(0)}{T_c} = 3.52. \quad (11)$$

In the single shell model at $T=0$ the two-quasiparticle energy $2E(0)$ is different from $2\Delta(0)$. Accordingly, two different ratios can be considered,

$$\frac{2E(0)}{T_c} = \frac{GM}{T_c} = \xi(n) \quad (12)$$

and

$$2\Delta(0)/T_c = 2\xi(n)\sqrt{n(1-n)}.$$

Both depend on the shell filling parameter n .

3 Averaging over the shell structure

The physical quantities we are interested in show rapid variations as functions of the electron number N , which are manifestations of the pronounced shell structure. We will average some quantities $f(n)$ over an interval of particle numbers N ,

$$(f(y))_{av} = \frac{1}{\gamma\sqrt{\pi}} \int f(x) \exp\left\{-\frac{(x-y)^2}{\gamma^2}\right\} dx,$$

where $x = N^{1/3}$ and $\gamma = 0.3$. The reason for averaging consists in following. Firstly, the number of electrons is not exactly known and there is a considerable uncertainty in the grain radius. In measurement on probes containing many grains, there will be an experimental N -distribution. Secondly, the phases of the fast N -oscillations are sensitive to small deviations from the ideal spherical symmetry of the adopted model. In real grains this symmetry is certainly broken by the roughness of the surface due to the discrete ionic background, by deviations of the shape from a sphere or hemisphere and by impurities. These imperfections will shift and wash out the oscillations. Averaging out the shell structure oscillations has also been advocated in ref. [12] studying the superconductivity of electrons in a cubic cavity as well as in the studies of the enhancement of paramagnetism in mesoscopic systems (cf. e. g. [19]).

The averaged values of $2E(0)/T_c$ are shown in Fig.4. They are larger than 4 because T_c is less than $T_c(n = 1/2)$ for $n \neq 1/2$ but $E(0)$ is n -independent. The averaged ratios of $2\Delta(0)/T_c$ are close to the bulk value 3.52 of a weakly coupled superconductor. Since the same ratio is also found for the cubic cavity [12] it may be of general nature.

4 Effective pairing strength in the BCS approximation

The two quasiparticle energy $2E(0)$ has been measured in refs. [9, 10] for different N at sufficiently low temperature, such that the zero temperature expressions can be applied. Within our single shell model, eq. (4) relates them directly to the coupling constant G . In

order to reproduce the experimental N - dependence of $2E(0)$ we must assume that $G(N)$ deviates from being $\propto 1/N$ as in the bulk. The restricted number of data points does not allow a quite definite determination of this function. We have adjusted two different phenomenological expressions,

$$G = gN^{-\alpha}, \quad g = 1.94 \text{ meV}, \quad \alpha = 0.47, \quad (13)$$

and

$$G = gN^{-1} \exp[-\alpha N^{-\beta}], \quad (14)$$

$$g = 3.21 \text{ eV}, \quad \alpha = 25, \quad \beta = 0.26$$

Since often transition temperatures are measured, we show in figs. 5a and 6a the values of T_c obtained by means of (12) and the expressions (13) and (13), respectively. For comparison, the values of $2E(0)$ measured in refs. [9, 10] are converted into "experimental" T_c values by means of eq. (12), using the averaged values of ξ .

As seen in Fig.5a, expression (13) is quite reasonable in the region of $N \sim 10^3 \div 10^5$. Varying α one can obtain T_c as an increasing ($\alpha < 1/3$) or decreasing ($\alpha > 1/3$) function of N . In the single shell model the particular role of $\alpha = 1/3$ is connected with the proportionality of T_c to GM i.e. to $GN^{1/3}$ (M averaged is $\sim N^{1/3}$).

The N - independent bulk coupling constant is given by $\lambda = G\rho_F$, where $\rho_F \propto N$ is the density of states at the Fermi-surface. Eq.(14) is constructed as a product of the bulk coupling constant and an N - dependent factor that accounts for the finite size effects. Accordingly, g is estimated using the coupling constant of bulk Al , $\lambda = g\rho_F N^{-1} = 0.4$ and the Fermi-gas density $\rho_F(Al)$. Both in eq.(14) and eq.(13) there are two fit parameters. Eq.(14) gives the correct asymptotic behavior of G at $N \rightarrow \infty$. The particular choice of the N -dependence corresponds to decreasing G at small N , which is reflected by the decrease of T_c and Δ at small N in Fig. 6. No physical significance is attributed to this decrease, because other choices of the N -dependence of the factor are possible.

The function $G(N)$ obtained by fitting the spherical model to the data strongly deviates from the bulk-law $G \propto N^{-1}$. It also deviates from the function $G(N)$ one would obtain within the frame work of models that disregard the shell structure, like the one of [4]. In order to illustrate this statement we assume equidistant levels near the Fermi surface with the spacing $d = \rho_F^{-1}$. This model is exposed e. g. in [22]. For $N > 10^4$, when $\Delta(0)/d \gg 1$, it is possible to replace the sums over the single electron levels by integrations and the well known expression

$$E(0) = \Delta(0) = \hbar\omega_D / \sinh\left(\frac{d}{G(N)}\right) \approx 2\omega_D \exp\left(-\frac{d}{G(N)}\right) \quad (15)$$

for the bulk is obtained. Expressing the pairing constant as the product $G(N) = d\lambda f(N)$, the factor $f(N)$ must grow with falling N in order to reproduce the experimental observed increase of Δ with decreasing N . This is at variance with our fits. In the case of eq. (13),

$f(N) = 0.6N^{0.53}$ and in the case of eq. (14), $f(N) = \exp(-25N^{-0.26})$, which both decrease with decreasing N .

Hence, if the shell structure in small grains is not taken into account, the effective coupling constant must be increased as compared to the bulk. On the other hand, in our spherical model the strong bunching of the electron already increases the value $\Delta(N)$ such that the coupling constant must be attenuated in order to account for the more modest increase seen in experiment. However, we do not consider our fits as evidence for a decrease of the coupling constant. Due to its high symmetry, the spherical model over-accentuates the shell structure. Imperfections of different nature will make the level bunching in real grains less pronounced. The spherical model and the model with equidistant levels may be considered as the two limiting cases of maximal and no shell structure, respectively. The real grains lie somewhere in between. It is quite reasonable to assume that their shell structure is weak enough such that $f(N)$ still increases with decreasing N .

In the context of the experimentally observed increase of T_c in thin films several effects have been discussed that lead to an increase of the coupling constant as a consequence of the reduced dimensionality [5, 11, 12, 13, 14, 15, 16, 17]. In particular, it has been pointed out that the surface phonon modes in films and small grains are expected to amplify the pair interaction. Our study shows that the electronic shell structure must be taken into account if these effects are quantitatively related to the experimentally observed increase of T_c , because the films often have a granular structure. Even for homogeneous films the quantization of the electron motion perpendicular to the surface must be taken into account, because ref. [2] has demonstrated that the pair gap Δ is considerably larger than its bulk value (15) when the thickness becomes as small as few times the Fermi wave length (assuming $G = \lambda\rho_F^{-1}$).

5 Critical temperature in finite systems

So far we have treated the pairing in the frame of the grand canonical ensemble. An important aspect of the small finite systems consists in the fact that the number of electrons in the grain is fixed and the canonical ensemble must be applied. In ref. [4] this question has been investigated on the basis of the generalized Landau - Ginzburg equations. This approach does not take into account the discreteness of the electron levels and their shell structure. The spherical model in single shell approximation is simple enough to carry through the canonical statistics including the shell structure.

As shown by Kerman [24], the pairing Hamiltonian can be expressed as the Casimir operator of the quasi spin algebra

$$H_p = -GA^+A; \quad A^+ = \sum a_t^+ a_{\bar{t}}^+; \quad [A, A^+] = M - N_{sh}$$

The eigenvalues $E_s^{(N)}$ are characterized by the quasi spin $Q_s = (M - s)/2$ or seniority,

which equals the number of unpaired particles in the shell,

$$E_s^{(N)} = -G \left[Q_s(Q_s + 1) - \left(\frac{M - N_{sh}}{2} \right)^2 - \frac{M - N_{sh}}{2} \right].$$

In this section we consider only the particles on the Fermi level, i. e. $N \equiv N_{sh}$. Each eigenvalue (except the ground state one, $Q_0 = M/2$) is degenerated with the multiplicity d_s :

$$d_s = \binom{2M}{s} - \binom{2M}{s-2}, \quad d_0 = 1$$

The single shell model gives the energy of two quasiparticle excitations (states with $s = 2$) equal to

$$E_2^{(N)} - E_0^{(N)} = G [Q_0(Q_0 + 1) - Q_2(Q_2 + 1)] = GM,$$

i.e. it is exactly the same value (4) as in *BCS*, where $GM = 2E(0)$. Thus, using the exact solution does not change the way to determine of G from the empirical two quasiparticle energies at $T \simeq 0$ [9, 10]. However, data on T_c in small grains require the consideration of the temperature dependence of the superconductivity in this model, which will be discussed below.

All thermodynamical quantities can be calculated from the canonical partition function Z , which is [25]

$$Z_N = \sum_{s=s_0}^N d_s \exp \{ -(E_s^{(N)} - E_0^{(N)})/T \},$$

where $s_0 = 0$ ($s_0 = 1$) and s are even (odd) integers if N is even (odd).

The absence of a sharp transition from superconducting to normal phase in finite systems can be demonstrated, for example, by studying the temperature dependence of the internal energy $\langle H \rangle$:

$$\langle H_p \rangle = \frac{1}{Z} \sum d_s E_s^{(N)} \exp \{ -(E_s^{(N)} - E_0^{(N)})/T \}. \quad (16)$$

It is frequently represented in the form analogous to the *BCS* expression:

$$\langle H_p \rangle = -\frac{\Delta_{can}^2}{G} - E_{ex}. \quad (17)$$

At $T = 0$, $\Delta_{can} = G \langle N + 2 | A^+ | N \rangle$, where $| N \rangle$ is the ground state function. It becomes Δ in the *BCS* approximation. E_{ex} is analogous to the exchange energy in *BCS* ($E_{ex}(BCS) = -G \sum \langle N_i \rangle^2$). There is an arbitrariness in the choice of this term in (17). In ref. [26] it is chosen such that for half filled shell ($N = M$) it is equal to $-GM/4$, which is the temperature independent *BCS* value in the single shell model. The choice

$$E_{ex} = \langle H_p \rangle |_{T \rightarrow \infty} = \frac{\sum d_s E_s^{(N)}}{\sum d_s} = -G \frac{N(N-1)}{2(2M-1)} \quad (18)$$

seems more appropriate to the problem, because for $T \rightarrow \infty$, where the pairing disappears, $\langle H \rangle$ given by (16) becomes equal to (18). The difference between (18) and $E_{ex}(BCS) = -GN^2/4M$ is negligible at large M and N . Inserting E_{ex} given by (18) into the expression (16) for $\langle H_p \rangle$, one gets for $T = 0$

$$\Delta_{can}(T = 0) = \Delta(0) \sqrt{1 + \frac{2}{2M - 1}}, \quad (19)$$

where $\Delta(0)$ is the *BCS* parameter given by (8). Thus, Δ_{can} is larger than $\Delta(0)$ at $T = 0$ but their ratio is practically equal to 1 for large M . The quantity Δ_{can} exceeds $\Delta(BCS)$ at any temperature, especially after T_c where $\Delta(BCS) = 0$. As seen in Fig. 7, it is smoothly decreasing and there is no sharp transition to the normal state. The larger M , the closer Δ_{can} approaches $\Delta(BCS)$.

The specific heat C of the electrons,

$$C = \frac{1}{N} T \frac{\partial^2}{\partial T^2} \{T \ln Z\} = \frac{1}{N} \frac{\partial}{\partial T} \langle H \rangle,$$

becomes in the single shell model

$$C = \frac{k}{N(T)^2} \left[\frac{1}{Z} \sum d_s (E_s^{(N)})^2 \exp\{-(E_s^{(N)} - E_0^{(N)})/T\} - \langle H_p \rangle^2 \right].$$

This equation can be represented in a G -independent form if we introduce the *BCS* critical temperature T_c as the unit of the temperature and energy,

$$\varepsilon_s = E_s^{(N)}/T_c, \quad t = T/T_c,$$

where T_c is determined by (10) for given M and N . As a consequence of T_c and E_s being proportional to G , one has

$$C = \frac{k}{Nt^2} \left\{ \frac{1}{Z} \sum d_s \varepsilon_s^2 \exp\left(-\frac{\varepsilon_s - \varepsilon_0}{t}\right) - \frac{1}{Z^2} \left[\sum d_s \varepsilon_s \exp\left(-\frac{\varepsilon_s - \varepsilon_0}{t}\right) \right]^2 \right\}. \quad (20)$$

In the grand canonical *BCS* approximation C can be represented as follows,

$$C = \frac{1}{N} \left[-\frac{\partial}{\partial T} \frac{\Delta^2}{G} \right].$$

In the case $N = M$ the *BCS* gap equation (5) takes the form ($t = T/T_c$)

$$\frac{\Delta}{\Delta(0)} = \tanh\left(\frac{\Delta}{\Delta(0)} \frac{1}{t}\right).$$

In the limits $T \rightarrow 0$ and $T \rightarrow T_c$ one obtains for the gap and specific heat:

$$t \ll 1: \quad \frac{\Delta}{\Delta(0)} = (1 - 2 \exp\{-2/t\}), \quad \frac{C(BCS)}{k} = \frac{8}{t^2} \exp\{-2/t\},$$

$$t \simeq 1 : \frac{\Delta}{\Delta(0)} = \sqrt{3(1-t)}, \quad \frac{C(BCS)}{k} = 3.$$

It is interesting to note that the jump in the $C(BCS)$ at $t = 1$ coincides with the value of the Gorter-Casimir two-fluid model [25].

Fig. 8 shows C calculated by means of (20). The case of the half filled shell $N = M$ is shown for several values of M . For comparison, the BCS result is added. Our model reproduces qualitatively the T dependence of C observed in small grains [8, 18]: when N decreases, the peak in C shifts to smaller t , it becomes lower and its width increases. A similar qualitative behavior of C was also obtained in the framework of the generalized Landau - Ginzburg model [4], and the two-level model system [24]. The similarity of the T dependence of C found in the three models, which are very different with respect to the shell structure of the electron levels, indicates that the behavior of the function $C(T)$ shown in Fig. 8 is a general consequence of the small and fixed number of particles. Fig.8 indicates that at $t = 1$ ($T = T_c$) the canonical specific heat in finite but not very small ($M > 10$) systems approximately attains the half of its maximum value. This observation correlates with empirical definition of T_c as the temperature at which a measured quantity takes 0.4 or 0.5 of its maximal value. This definition was used in measurements of both electronic specific heats [8, 18] and electromagnetic quantities [17, 18]. The critical temperatures determined this way practically coincide. Thus, the consideration of the theoretical specific heat in the single shell model canonical approach shows that the critical temperature calculated in the grand canonical BCS approximation can be adopted as the transition temperature T_c for small systems. Our determination of the coupling constant G performed in the previous section on the basis of measured energies of two quasiparticle excitations and critical temperatures practically require no corrections.

6 Magnetic susceptibility

The magnetic susceptibility χ of the electrons in the low field limit is given by the change of their thermodynamic potential

$$\Omega(T, B) = \langle H - \mu N + \omega_L(L_z + 2S_z) + \frac{m\omega_L^2}{2}(x^2 + y^2) \rangle - TS \quad (21)$$

with respect to the external magnetic field B (assumed to be in direction of the z - axis),

$$\chi = -\frac{1}{V} \frac{\partial^2 \Omega}{\partial B^2} \Big|_{B=0}. \quad (22)$$

We have introduced the Larmor frequency $\omega_L = \mu_B B$, where μ_B and m are the Bohr magneton and electron mass, respectively. Here, $H - \mu N$ is the pairing hamiltonian (1), L_z the z -component of the orbital angular momentum, S_z the z -component of the spin, V the volume and S the entropy of the system. The single electron levels are Zeeman-split

by the magnetic field,

$$\varepsilon_t(B) = \tilde{\varepsilon}_t + \omega_L(\Lambda_t + 2\Sigma_t), \quad (23)$$

$$\tilde{\varepsilon}_t = \varepsilon_t^{(0)} + \frac{m\omega_L^2}{2} \langle t | x^2 + y^2 | t \rangle. \quad (24)$$

The z -projections of the orbital and spin momentum are denoted by Λ_t and Σ_t . The gyromagnetic factor of the electron is set to 2 and $\varepsilon_t^{(0)} = \tilde{\varepsilon}_t(B = 0)$.

For spherical systems

$$\langle t | x^2 + y^2 | t \rangle = \frac{2}{3} \langle t | r^2 | t \rangle$$

and the expression for Ω can be reduced to the following form:

$$\Omega = 2 \sum_{t>0} (\tilde{\varepsilon}_t - \mu - e_t) + \Delta^2/G - 2T \sum_{t,\Lambda>0} \log [(1 + \exp(-E_t/T))(1 + \exp(-E_{\bar{t}}/T))], \quad (25)$$

$$E_t = e_t + \omega_L(\Lambda_t + 2\Sigma_t), \quad E_{\bar{t}} = e_t - \omega_L(\Lambda_t + 2\Sigma_t),$$

$$e_t = \sqrt{(\tilde{\varepsilon}_t - \mu)^2 + \Delta^2}, \quad \Delta = 2G \sum_{t,\Lambda>0} u_t v_t (1 - f_t - f_{\bar{t}}),$$

$$f_t = (1 + \exp(E_t/T))^{-1}, \quad f_{\bar{t}} = (1 + \exp(E_{\bar{t}}/T))^{-1}.$$

For normal grains ($G = 0$) the first two terms in Eq.(25) vanish and E_t is replaced by $\tilde{\varepsilon}_t - \mu$. Inserting (24) and (25) into (22), one obtains the grand canonical susceptibility of a spherical grain,

$$\chi = \chi_D + \chi_P,$$

as a sum of a diamagnetic and a paramagnetic contribution, χ_D and χ_P , respectively.

The diamagnetic contribution is given by

$$\chi_D = \frac{8\mu_B^2 m}{3V\hbar^2} \sum_{t,\Lambda>0} \langle t | r^2 | t \rangle n_t. \quad (26)$$

The occupation numbers n_t are for $G > 0$

$$n_t = \frac{1}{2} \left\{ 1 - \frac{\varepsilon_t^{(0)} - \mu}{e_t^{(0)}} (1 - 2f_t) \right\} \quad (27)$$

$$e_t^{(0)} = \sqrt{(\tilde{\varepsilon}_t^{(0)} - \mu)^2 + \Delta^2}, \quad f_t = (1 + \exp\{e_t^{(0)}/T\})^{-1} \quad (28)$$

and for $G = 0$

$$n_t = f_t, \quad f_t = (1 + \exp\{(\varepsilon_t^{(0)} - \mu)/T\})^{-1}. \quad (29)$$

The matrix element in (26) can be straightforwardly calculated with Bessel functions, which are eigenfunctions of our model,

$$\langle t | r^2 | t \rangle = \frac{R^2}{2} \left\{ \frac{1}{2} + \frac{(l + 1/2)^2 - 1}{(kR)^2} \right\} t. \quad (30)$$

Here, k is the wave number of state t . In the single shell approximation the pairing acts only in the last shell. Since $\langle t | r^2 | t \rangle$ is constant within one shell, $r^2 \propto N$ and equal to its value without pairing. Hence, $\chi_D(G, T)$ is given by (26) calculated for $G = 0$.

The paramagnetic contribution,

$$\chi_P = \frac{\mu_B^2}{VT} \sum_{t, \Lambda, \Sigma} f_t(1 - f_t)(\Lambda_t + 2\Sigma_t)^2 = \frac{2\mu_B^2}{VT} \sum_{t, \Lambda} f_t(1 - f_t)(\Lambda_t^2 + 1), \quad (31)$$

is very sensitive to the pairing and the shell structure. Again, we consider small temperatures ($T < T_c$), such that the level spacing near the Fermi level is much larger than T , and calculate χ_P by means of the single shell model. Taking into account that for the level with the number of magnetic substates $M = 2l + 1$,

$$\sum \Lambda^2 = \frac{l(l+1)(2l+1)}{3} = \frac{(M^2 - 1)M}{12},$$

we obtain for χ_P

$$\chi_P(G = 0, T) = \frac{\mu_B^2}{6VT} n(1 - n)M(M^2 + 11), \quad n = N_{sh}/2M, \quad (32)$$

$$\chi_P(G > 0, T) = \frac{\mu_B^2}{6VT} n(1 - n)M(M^2 + 11) \left[1 - \left(\frac{\Delta(T)}{\Delta(0)} \right)^2 \right]. \quad (33)$$

As seen, the single shell model expressions for χ_P can be written such that the influence of the pairing is expressed by a separate factor:

$$\chi_P(G > 0, T) = \chi_P(G = 0, T) \left(1 - \left(\frac{\Delta(T)}{\Delta(0)} \right)^2 \right). \quad (34)$$

The temperature dependence of χ is displayed in Fig.10, which shows the case $N = 3371$, corresponding to the middle of the shell, where χ_P has its maximum. For $T \rightarrow 0$ the paramagnetic susceptibility goes to zero. Hence, the grain becomes an ideal diamagnet. The reason is the same as for an atom. The first excited state is at the energy $2E(0) \gg T$. i. e. only the diamagnetic part (26) contributes. The susceptibility for the non-superconducting system $\chi_P(G = 0, T)$ diverges, because it costs no energy to occupy the magnetic substates such that the magnetic moment is finite. Hence, at small temperatures the susceptibility of superconducting grains is negative. It increases with the temperature, changes sign and reaches its maximum at $T = T_c$. Then it decreases again proportional to $1/T$.

At low temperatures $T \sim (0.1 \div 0.2)T_c$, the susceptibility for the unpaired state, $\chi(G = 0)$, takes large paramagnetic values in the open shells [21, 28]. This is an example of the general appearance of paramagnetism in a confined electron system, which is reviewed e. g. in [19]. Evidence for this paramagnetic enhancement in mesoscopic normal systems has been found [29]. In our case $\chi(G = 0)$ is about 10 times higher than $\chi(G > 0)$.

Thus, measuring χ at these temperatures can give information whether a grain is normal or superconducting.

Averaged values of χ as a function of $N^{1/3}$ are shown in Fig.11. Both cases $G = 0$ and $G > 0$ are displayed for $T = 3$. The averaged values of $\chi(G = 0)$ fluctuate around some constant. At $T = 3K$, which is higher than $T_c(bulk)$, many of grains in the range $10^3 < N < 10^5$ are superconductors. Hence, the averaged values of $\chi(G > 0)$ are less than $\chi(G = 0)$. For $N > 10^5$ the susceptibility $\chi(G > 0)$ approaches $\chi(G = 0)$. The finite size effects, which make the small grains superconducting at $T = 3K$, are no longer strong enough to sustain the superconducting state. For $N^{1/3} < 15$, the two different N dependences of G are reflected by the susceptibility: if G grows with decreasing N according to (13), χ decreases (curve 2). If it decreases according to (14), χ increases and reaches $\chi(G = 0)$. Therefore, the measurement of the N -dependence of the susceptibility at low temperatures ($T < T_c$) could give valuable information concerning the N -dependence of G .

Let us now derive the susceptibility for the canonical ensemble. In the presence of a magnetic field B the degeneracy of states with a definite seniority s is lifted, i. e.

$$\delta E(B, s, L, S, \Lambda, \Sigma) = \omega_L(\Lambda_s + 2\Sigma_s) + \frac{\omega_L^2 m}{2} \langle sLS | \frac{2}{3} r^2 | sLS \rangle. \quad (35)$$

As before, $L_s, S_s, \Lambda_s, \Sigma_s$ are the orbital and spin momenta and their projections, respectively. The subscript s indicates that these momenta correspond to a fixed seniority s and that they are chosen to be consistent with the Pauli principle.

In the single shell approximation, χ_D is given by (26) calculated for $G = 0$. The reason is the same as for the grand canonical ensemble. The paramagnetic contribution can be written in a G -independent form like the canonical heat capacity if we introduce the BCS critical temperature T_c as the unit of the temperature and energy,

$$\chi_P = \frac{\mu_B^2}{ZT} \sum_s \exp\left(-\frac{\varepsilon_s - \varepsilon_0}{t}\right) R_s, \quad (36)$$

$$R_s = \sum_{L_s, S_s, \Lambda_s, \Sigma_s} (\Lambda_s + 2\Sigma_s)^2, \quad (37)$$

$$\varepsilon_s = E_s^{(N)}/T_c, \quad t = T/T_c, \quad (38)$$

To calculate the canonical χ_P one needs the values of the orbital and spin momenta at a given seniority. This problem is solved in the Appendix.

The results for the shells with $l = 2$ and $l = 5$ are shown in Fig.12 in comparison with the grand canonical calculations. The relationship (33), which is exact for the grand canonical ensemble, holds with high accuracy also in the case of the canonical ensemble if the grand canonical Δ is replaced by the canonical Δ_{can} . It permits a transparent interpretation of the modification of the susceptibility due to the conservation of the particle number. The consequences of the superconductivity are expressed by the factor $1 - (\Delta_{can}(T)/\Delta(0))^2$. The canonical approach washes out the sharp boundary between superconducting and normal

states. As illustrated in fig. 7, the canonical gap disappears gradually. Correspondingly, the transition from superconducting and normal values of the susceptibility is smoothed. The exact calculation supports this conclusion.

7 Conclusions

We have studied the dependence of the pair correlations on the particle number N in Al nanometer-scale grains, $10^3 < N < 10^5$. Using the spherically symmetric infinite well as a model of the field, we have calculated the gap parameter Δ as functions of N . Comparing it with experimental data from tunneling experiments, the pairing coupling constant $G(N)$ is fixed as function of the number of electrons N .

In our model, the bunching of the electron levels (shell structure) strongly enhances the pair correlations in the small grains. This enhancement is so strong that fitted coupling constant $\lambda(N) = G(N)\rho_F$ *decreases* with decreasing N , in order to account for the more modest increase seen in experiment. We interpret this as a consequence that our spherical model has too pronounced a shell structure. The bunching of the electronic levels in realistic grains is most likely weaker due to deviations of the shape from the ideal sphere, surface roughness and impurities, Thus, the enhancement of the superconductivity due to the shell structure is expected to be weaker and a different function $\lambda(N)$ will fit the experimental data on $\Delta(N)$, which for the limiting case of no shell structure *increases* with decreasing N .

The enhancement of the pair correlations by the shell structure should be considered as a mechanism that exists in addition to the increase of the effective pair coupling constant λ caused by the modification of the phonon spectrum in small grains. The completely different N dependence of λ found for the spherical and structureless models demonstrates that a careful estimate of the shell structure in realistic grains is needed in order to determine the N - dependence coupling constant from the data.

The averaged magnetic susceptibility for the spherical grains in the normal state turns out to be strongly paramagnetic. Evidence for this paramagnetic enhancement in mesoscopic normal systems has been found [29]. In our spherical model the superconductivity strongly reduces the paramagnetism, but the susceptibility remains large and positive. Thus, the surprising prediction is that small superconductors may be paramagnetic. In realistic grains with a less pronounced shell structure the pair correlations may be strong enough to make the susceptibility negative. Our study shows that the susceptibility of grains composed of superconducting material results from an intricate interplay between the pair correlations and the spatial confinement of the electrons.

The properties of the superconducting grains with the number of atoms below 10^5 are significantly modified by the fixed number of electrons. Instead of a sharp phase transition an extended transition region in temperature appears. A transition temperature can be defined as the value where the the specific heat shows the most rapid drop. This

critical temperature agrees rather well with T_c calculated in the grand canonical *BCS* approximation and can be adopted as the transition temperature T_c for small systems.

Part of this work was performed during the visit of two authors (N.K. and V.M.) to Forschungszentrum Rossendorf. They thank Prof. Prade for hospitality. This work is supported by the INTAS (grant INTAS-93-151-EXT).

8 Appendix

The sum R_s appearing in Eq.(37) amounts to the difference of the sums of squares of orbital and spin momentum projections corresponding to states with $N = s$ and $N = s - 2$ particles,

$$R_s = R_{N=s} - R_{N=s-2} \quad (39)$$

$$R_N = \sum_i \langle \psi_i^N | (\hat{L}_z + 2\hat{S}_z)^2 | \psi_i^N \rangle$$

R_N includes the expectation values of the z -projection orbital and spin momentum operators (\hat{L}_z and \hat{S}_z). The total number of states ψ_i^N at a given N is

$$\binom{2M}{N}, \quad M = 2l + 1,$$

with l being the orbital momentum. In what follows we assume that N is even and equal to $2k$. As known [30], the exclusion principle requires that orbital momentum and spin functions entering into ψ_i are basic vectors of conjugate or dual representations of the permutation group and their Young diagrams should correspond to each other by exchange of rows and columns. The diagrams of spin functions consist of $k + S$ squares in the first row and $k - S$ in the second one. S is the spin taking the only value for each diagram and ranging from 0 to $k = N/2$ for a fixed even integer N . The orbital permutation symmetry is characterized by two column diagrams, the whose length of columns is equal to $k + S$ and $k - S$. In general, such diagrams involve several states with orbital momenta L_{kS} . We assume that ψ_i^N is a direct product of an orbital function $\varphi(k, S, L_{kS}, \Lambda)$ and a spin one $\chi(S, \Sigma)$ where Λ and Σ are eigenvalues of the operators \hat{L}_z and \hat{S}_z respectively.

$$R_{N=2k} = \sum_{L_{kS}, S, \Lambda, \Sigma} \langle \varphi(k, s, L_{kS}) \chi(S, \Sigma) | (\hat{L}_z + 2\hat{S}_z)^2 | \varphi(k, s, L_{kS}) \chi(S, \Sigma) \rangle \quad (40)$$

As the sums over Λ and Σ are independent, R_N can be divided into orbital and spin parts:

$$R_N = R_N^\Lambda + R_N^\Sigma, \quad (41)$$

$$R_{N=2k}^\Lambda = \sum_{L_{kS}, S} \langle \varphi(k, s, L_{kS}) | \hat{L}_z^2 | \varphi(k, s, L_{kS}) \rangle (2S + 1), \quad (42)$$

$$R_{N=2k}^\Sigma = \sum_{S, \Sigma} \langle \chi(S, \Sigma) | 4\hat{S}_z^2 | \chi(S, \Sigma) \rangle d_{kS} = \frac{4}{3} \sum_{S=1}^k S(S+1)(2S+1) d_{kS}, \quad (43)$$

where d_{kS} is the dimension of the orbital space with the permutation symmetry described by the two column Young diagrams mentioned above.

$$d_{kS} = \binom{M+1}{k-S} \binom{M+1}{k+S} \frac{2S+1}{2M+1} \quad (44)$$

$$\sum_{S=0}^k (2S+1)d_{kS} = \binom{2M}{2k} \quad (45)$$

Eq.(43) indicates that R_N^Σ can be computed straightforwardly whereas finding R_N^Λ needs the determination of the set of L_{kS} .

This task can be removed by taking into account that external product of two completely antisymmetric functions $\tilde{\varphi}(k+S, L, \Lambda)$ ($k+S$ squares in the only column of the Young diagram) and $\tilde{\varphi}(k-S, L', \Lambda')$ ($k-S$ squares) gives rise to a series of basic vectors of irreducible representations with two column diagrams. Each vector arises only once and the lengths of columns vary from $(k+S, k-S)$ up to $(2k, 0)$, i.e. the decomposition of this external product contains $\varphi(k, S', L_{kS}, \Lambda)$ functions with $S'_{min} = S$ and $S'_{max} = k$. This decomposition permits to reduce Eq.(42) to the following

$$R_{N=2k}^\Lambda = \sum_{S=0}^k \sum_{L, \Lambda} \left\{ \langle \tilde{\varphi}(k+S, L, \Lambda) | \hat{L}_z^2 | \tilde{\varphi}(k+S, L, \Lambda) \rangle \binom{M}{k-S} + \langle \tilde{\varphi}(k-S, L, \Lambda) | \hat{L}_z^2 | \tilde{\varphi}(k-S, L, \Lambda) \rangle \binom{M}{k+S} \right\} (2 - \delta_{S,0}) \quad (46)$$

The orbital momenta L of $\tilde{\varphi}$ have to be compatible with antisymmetry of these states. This points out an elementary way to compute them by summing single particle projections among which should not be identical ones.

References

- [1] J.A.A.J. Perenbom, P.Wyder and F.Myer, Phys. Rep. **78**,174(1981).
- [2] J. M. Blatt and C. J. Thompson, Phys. Rev. Lett. **10**, 332 (1963)
- [3] R.H.Parmenter, Phys. Rev. **166**,392(1968).
- [4] B.Mühlschlegel, D.J.Scalpino, R.Denton, Phys.Rev., **B6**,1767(1972).
- [5] S.Matsuo, H.Suigiura and S.Noguchi, J. Low Temp. Phys.,**15**,481(1974).
- [6] B.Abeles, R.W.Cohen and G.W.Cullen, Phys. Rev. Lett. **17**,632(1966).
- [7] R.W.Cohen, B.Abeles, Phys. Rev. **168**,443(1968).
- [8] T.Tsuboi, T.Suzuki, J. Phys. Soc. of Japan **42**,437(1977).
- [9] D.C.Ralf, C.T.Black, and M.Tinkham, Phys. Rev. Lett. **74**,3241(1995).
- [10] C.T.Black, D.C.Ralf and M.Tinkham, Phys. Rev. Lett. **76**,688(1996).
- [11] A.W.Anderson, J. Phys. Chem. **11**,26(1959).
- [12] E.A.Shapoval, JETP Lett. **5**,45(1967).
- [13] A.Rothwarf, Phys. Lett. **30A**,55(1969).
- [14] H.P.Watson, Phys. Rev. **B2**,1282(1970).
- [15] M.Strongin, R.S.Thompson, O.F.Kammerer, J.E.Cow, Phys. Rev. **B1**,1078(1970).
- [16] J.Standish, R.L.Pompi, Phys. Rev. **B21**,5185(1980).
- [17] C.R.Leavens, E.W.Fenton, Phys. Rev. **B24**,5080(1981).
- [18] R.L.Filler, R.Lindenfeld, T.Worthington, Phys. Rev. **B21**,5031(1980).
- [19] K. Richter, D. Ullmo, R. A. Jalabert, Phys. Rep. **276** (1996), 1
- [20] S. Frauendorf, S. Reimann and V. V. Pashkevich, Surf. Sci. Rev. and Lett. **3**, 441 (1996)
- [21] S.Frauendorf, V.M.Kolomietz, A.G.Magner and A.I.Sanzhur, Phys. Rev. **B**, in print; preprint physics/9807002
- [22] P.Ring, P.Schuck, The Nuclear Many Body Problem (Springer,Berlin,1980).
- [23] A.L.Goodman, Nucl. Phys. **A352**,30(1981).

- [24] A.K.Kerman, Ann. Phys. **12**,300(1961).
- [25] C.Esebbag, J.L. Edigo, Nucl. Phys. **A552**,205(1993).
- [26] 2R.Rossignoli, N.Canosa, P.Ring, Nucl. Phys. **A591**,15(1995).
- [27] C.J.Gorter, H.B.G.Casimir, Physik. Z. **35**,963(1934), Z. techn. Physik **15**,539(1934).
- [28] J.M. van Ruitenbeek, D.A. van Leeuwen, Phys. Rev. Lett. **67**,640(1991).
- [29] L. P. Lévy, D. H. Reich, L. Pfeiffer and K. West, Physica **B 189**, 204 (1993)
- [30] M. Hamermesh, Group theory and its application to physical problem. (Addison-Wesley publishing company,1964)

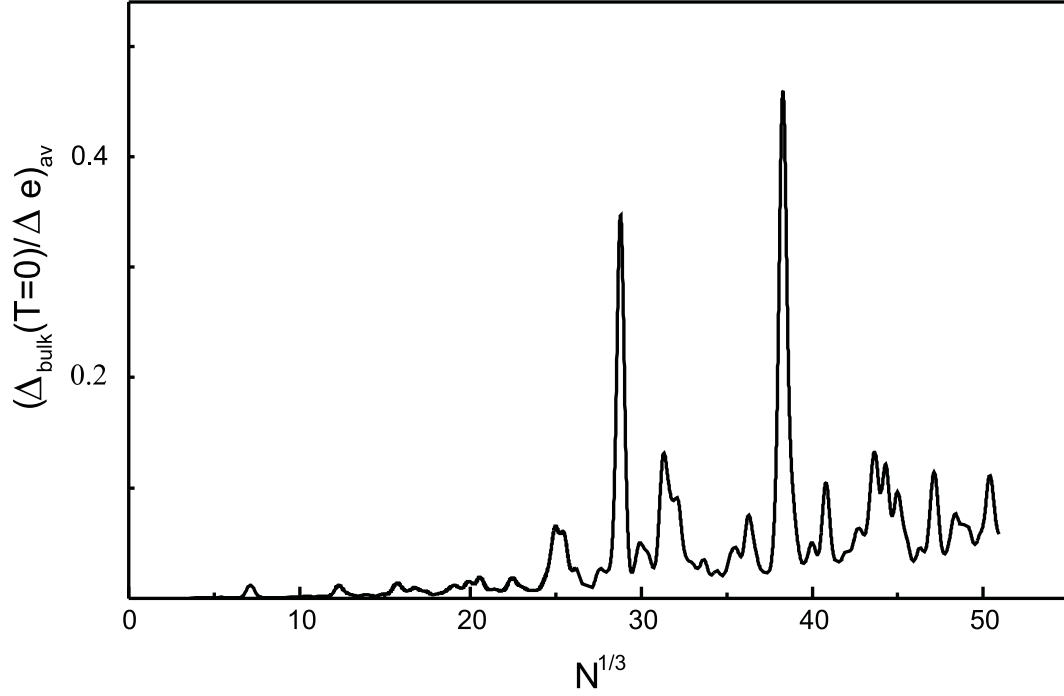


Figure 1: Averaged values of $\Delta_{bulk}(T=0)/\Delta e$ v.s. $N^{1/3}$. The pairing gap of bulk Al is $\Delta_{bulk}(T=0)$ and $\Delta e = e_{F+1} - e_F$. e_F, e_{F+1} are energies of the Fermi level and the next higher one. The meaning of the averaging is explained at the end of section 3.

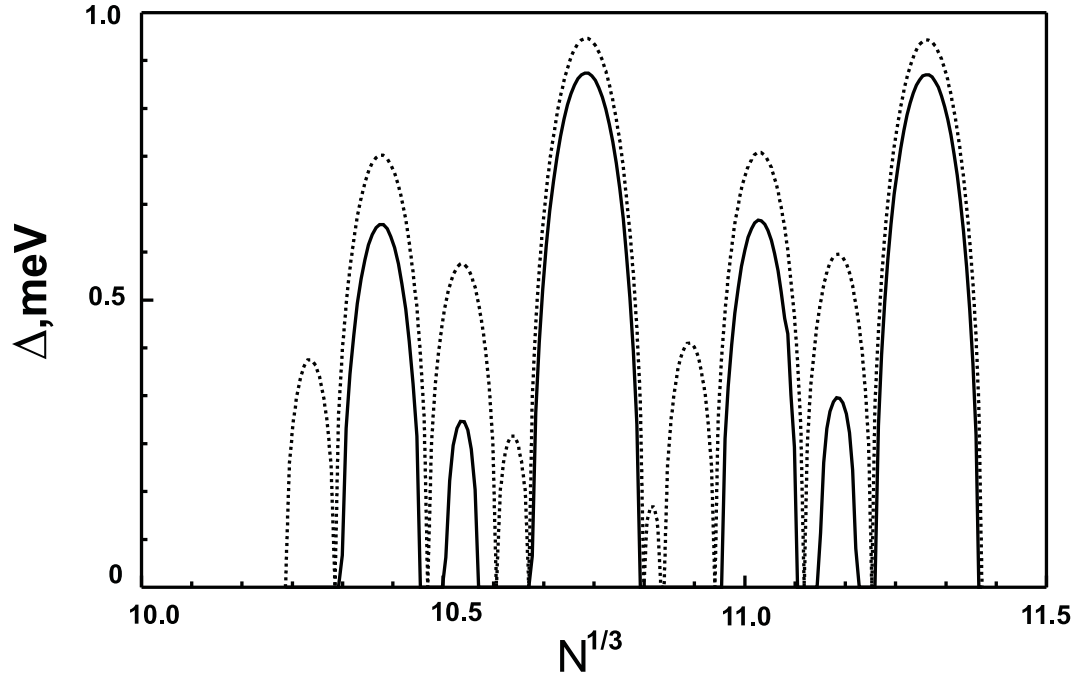


Figure 2: Pairing gap $\Delta(T, N)$ v.s. $N^{1/3}$. Dashed lines: $T = 0$, solid lines: $T = 3$ K.

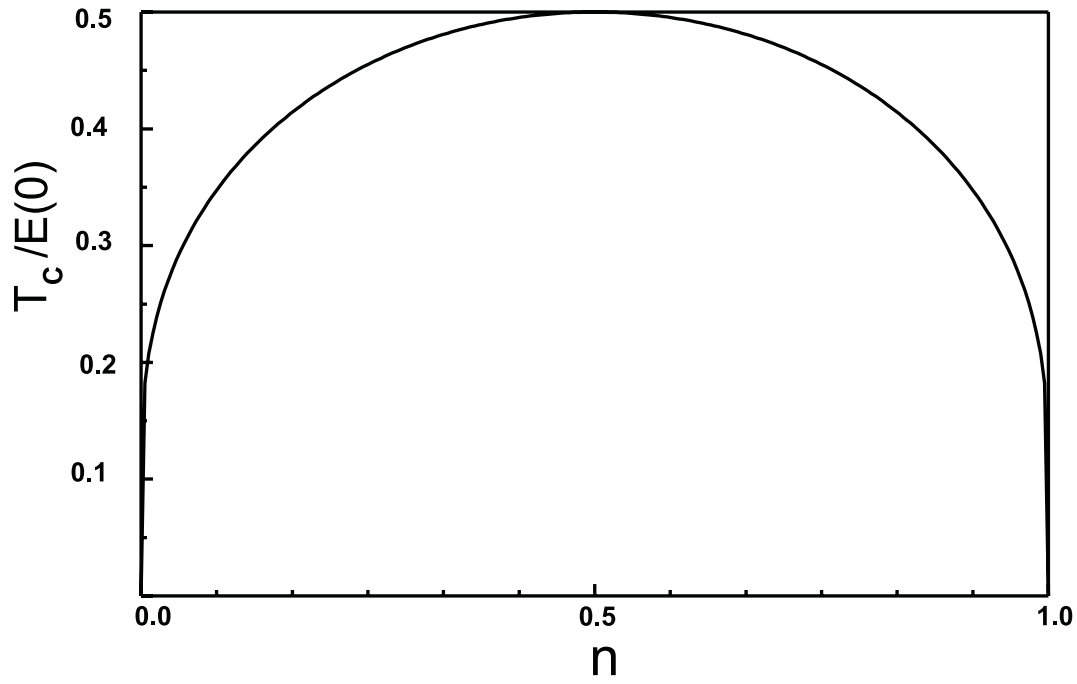


Figure 3: $T_c/E(0)$ v.s. the occupation degree of the shell $n = N_{sh}/2M$.

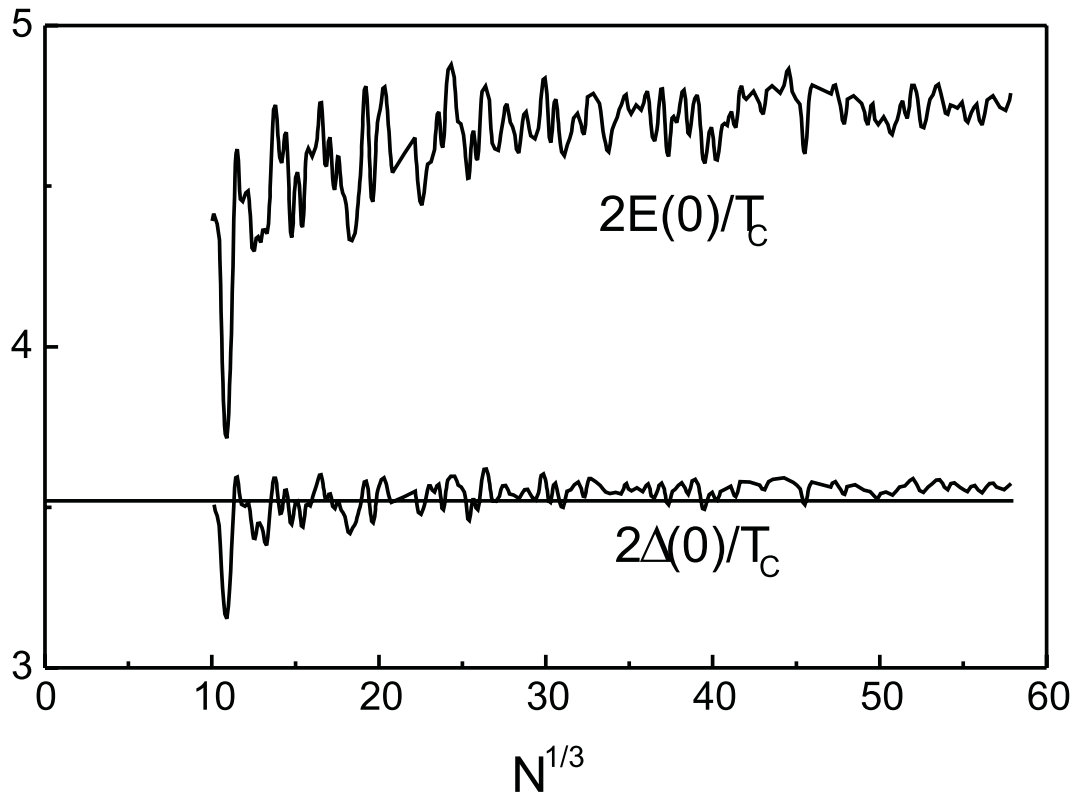


Figure 4: Averaged values of $2E(0)/T_c$ and $2\Delta(0)/T_c$ v.s. $N^{1/3}$.

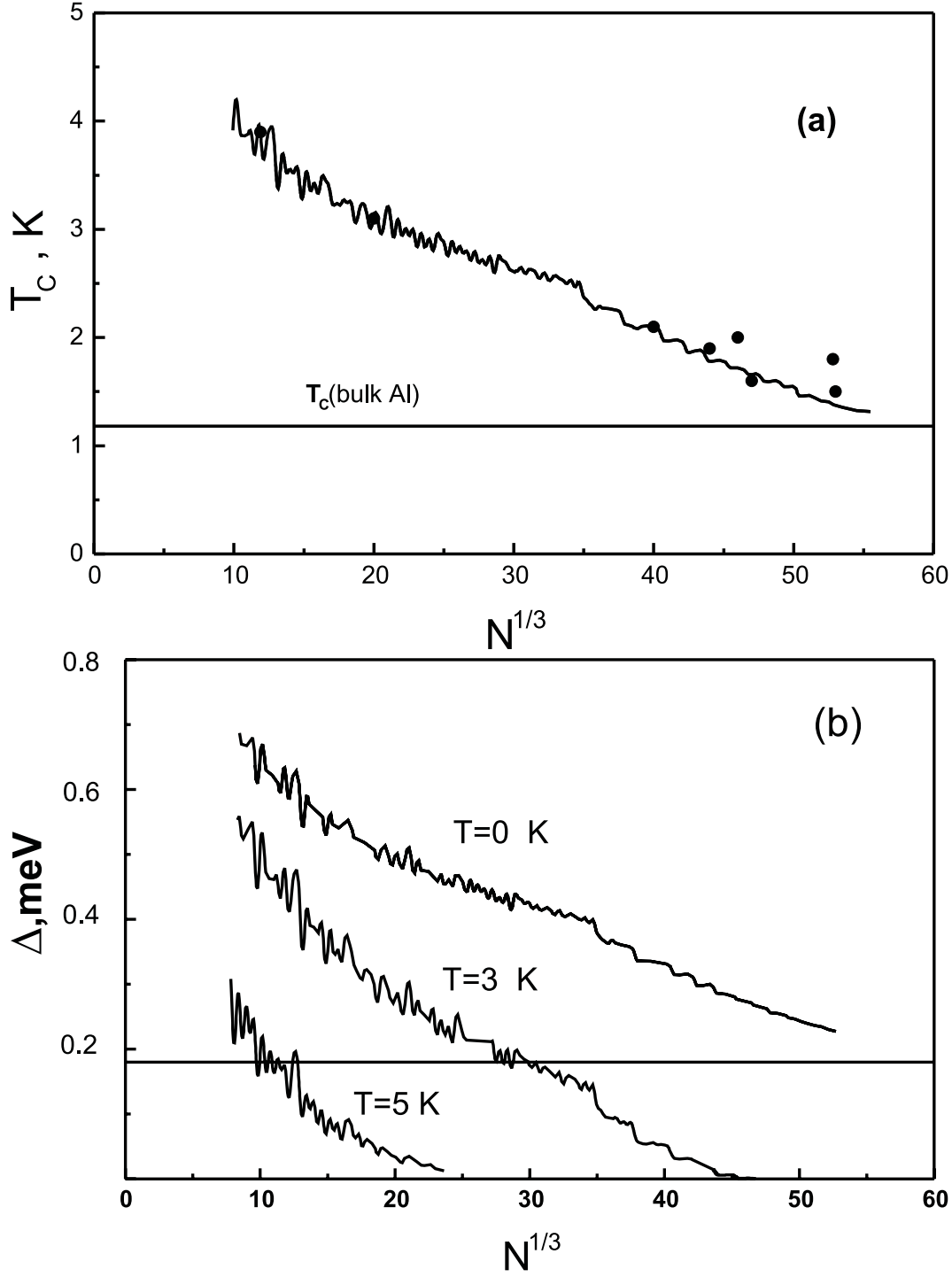


Figure 5: (a) T_c v.s. $N^{1/3}$. Points represent experimental data [8, 9] on Δ , which are converted by mean of eq. (12) into T_c . The solid line is the averaged T_c calculated with $G = 1.94N^{-0.47} \text{ meV}$. (b) Averaged pairing gap v.s. $N^{1/3}$ calculated at $T = 0, 3 \text{ K}$ and 5 K . The horizontal line gives $\Delta(0)$ of bulk Al .

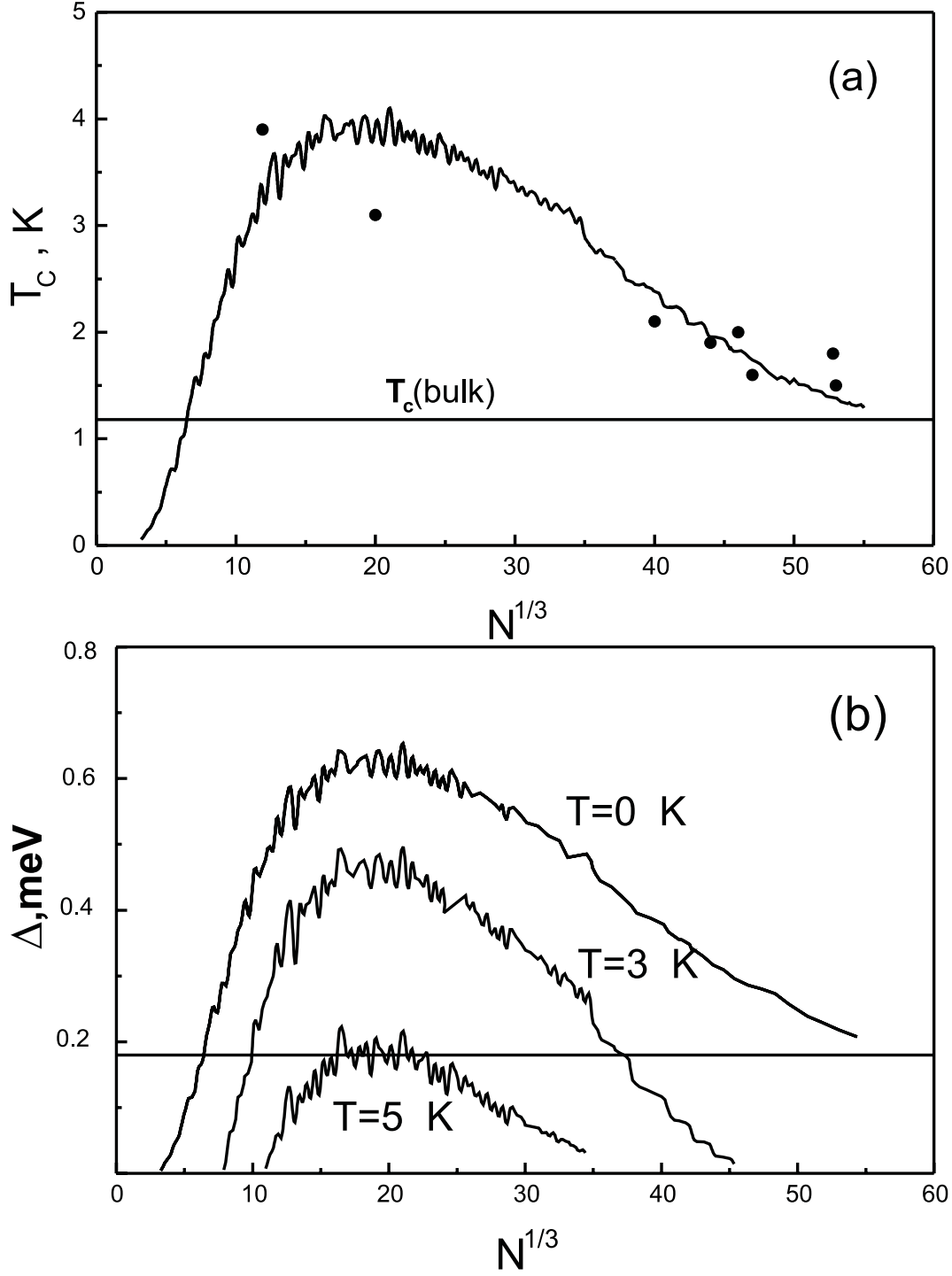


Figure 6: (a) T_c v.s. $N^{1/3}$. Points represent experimental data [8, 9] on Δ , which are converted by mean of eq. (12) into T_c . The solid line is the averaged T_c calculated with $G = 3.21N^{-1} \exp(-25N^{-0.26})$ eV. (b) See the caption in 5b.

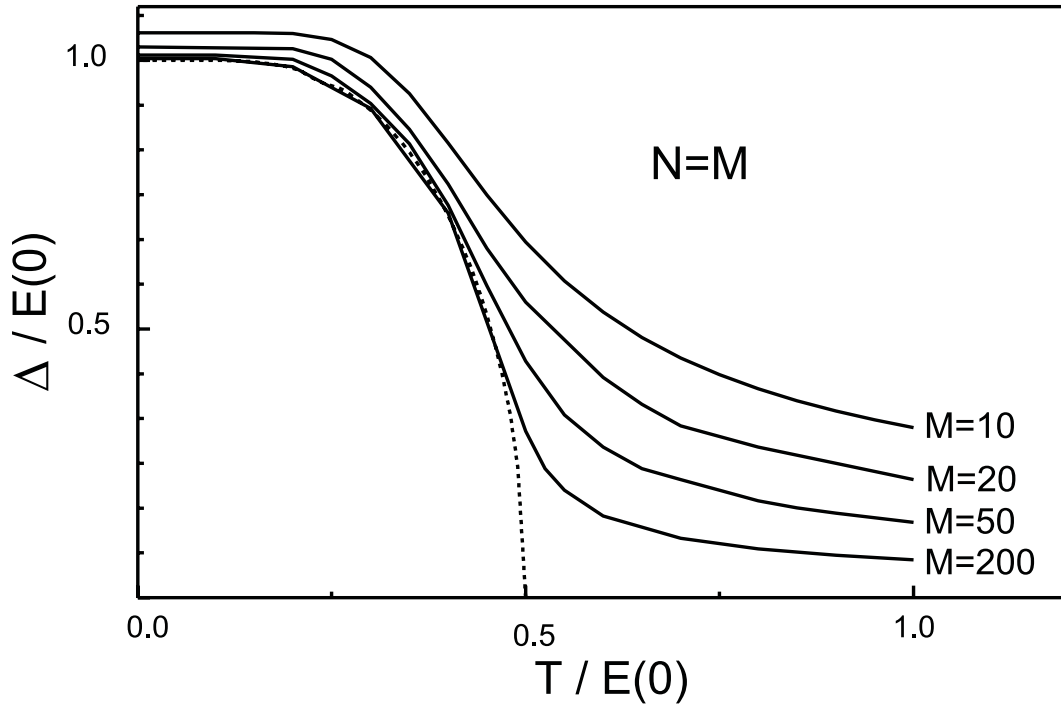


Figure 7: Pairing gaps calculated v.s. T/T_c at different values of M for the half filled shell. Solid and dashed lines correspond to canonical and *BCS* results, respectively.

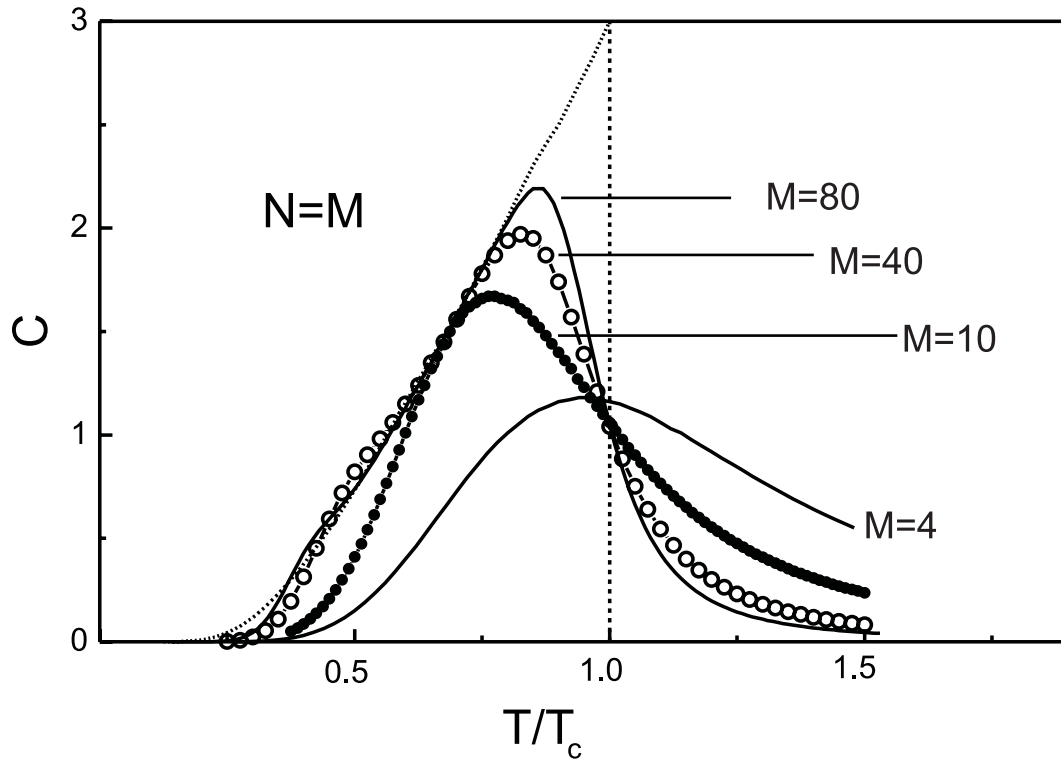


Figure 8: Specific heat C of the single shell v.s. T/T_c at different M . Solid and dashed lines correspond to canonical and *BCS* results, respectively.

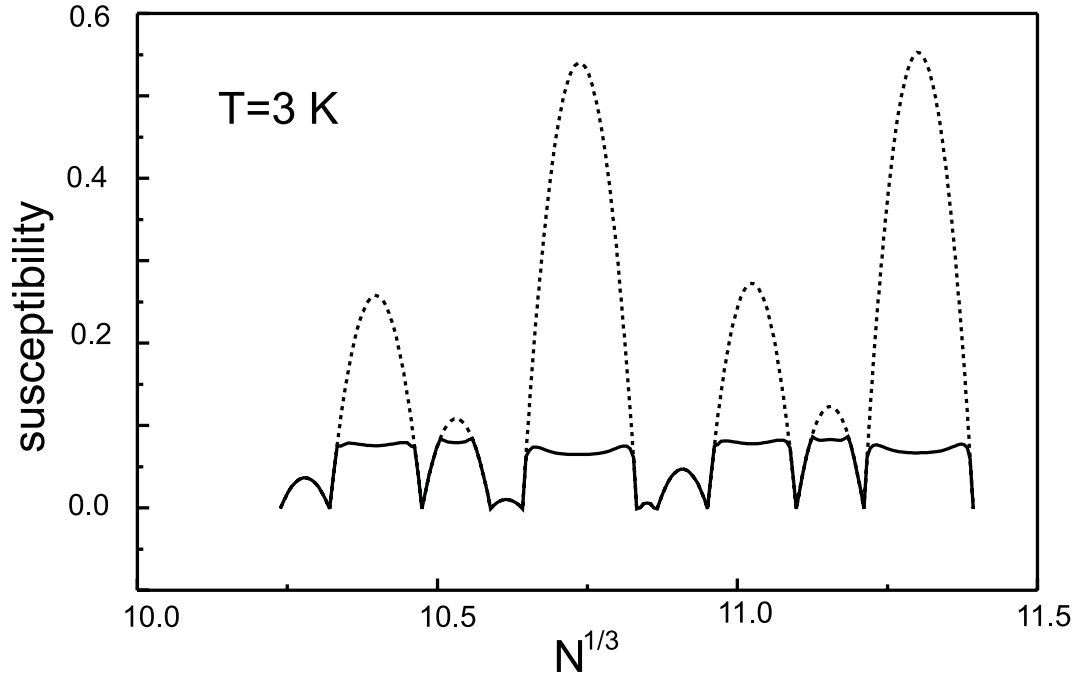


Figure 9: Susceptibility (in units $|\chi_L| \cdot 10^5$ where χ_L is the Landau expression for diamagnetism of the degenerate free electron gas) v.s. $N^{1/3}$. Dashed lines: $G = 0$, solid lines: $G > 0$.

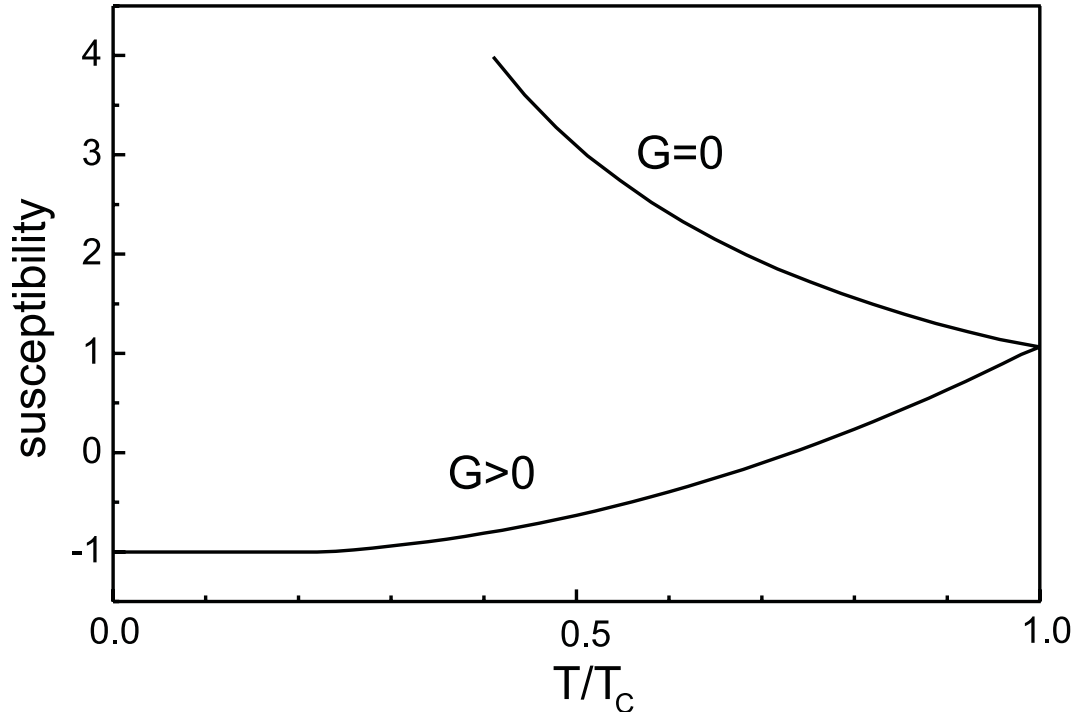


Figure 10: Susceptibility (in units $|\chi_D|$ ($G = 0, T = 0$)) v.s. T/T_c . Dashed and solid lines give χ at $G = 0$ and $G > 0$, respectively.

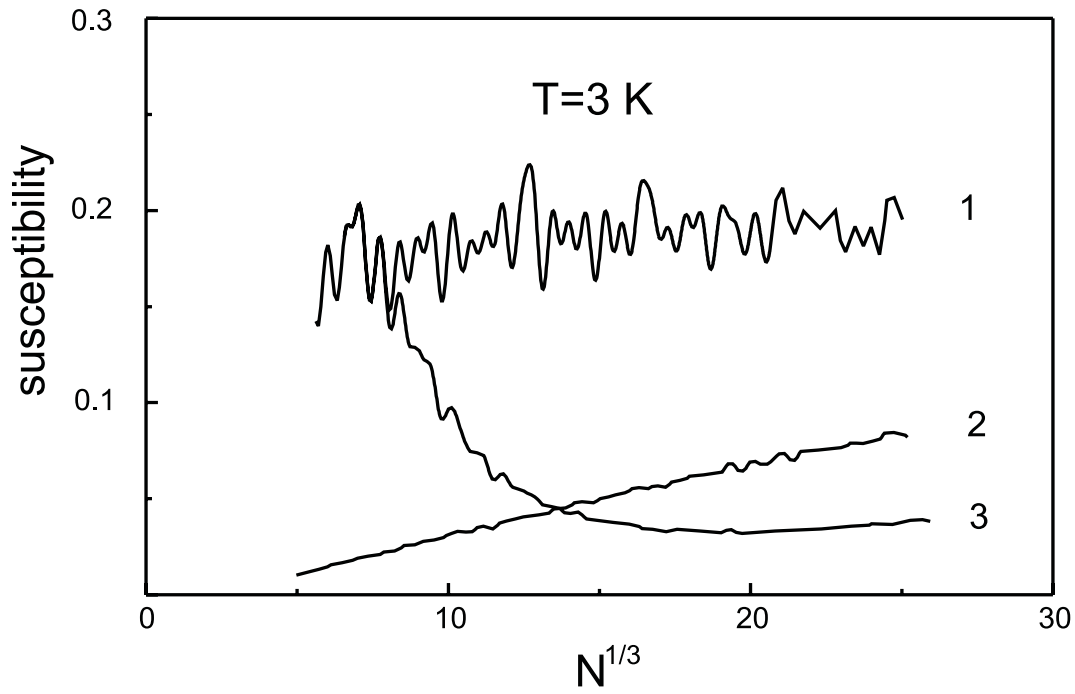


Figure 11: Averaged susceptibility (in units $|\chi_L| \cdot 10^5$) v.s. $N^{1/3}$ at $T = 3$ K. Curves 1, 2, 3 correspond to $G = 0$; $G = 1.94N^{-0.47}$ meV; $G = 3.21N^{-1} \exp(-25N^{-0.26})$ eV, respectively.

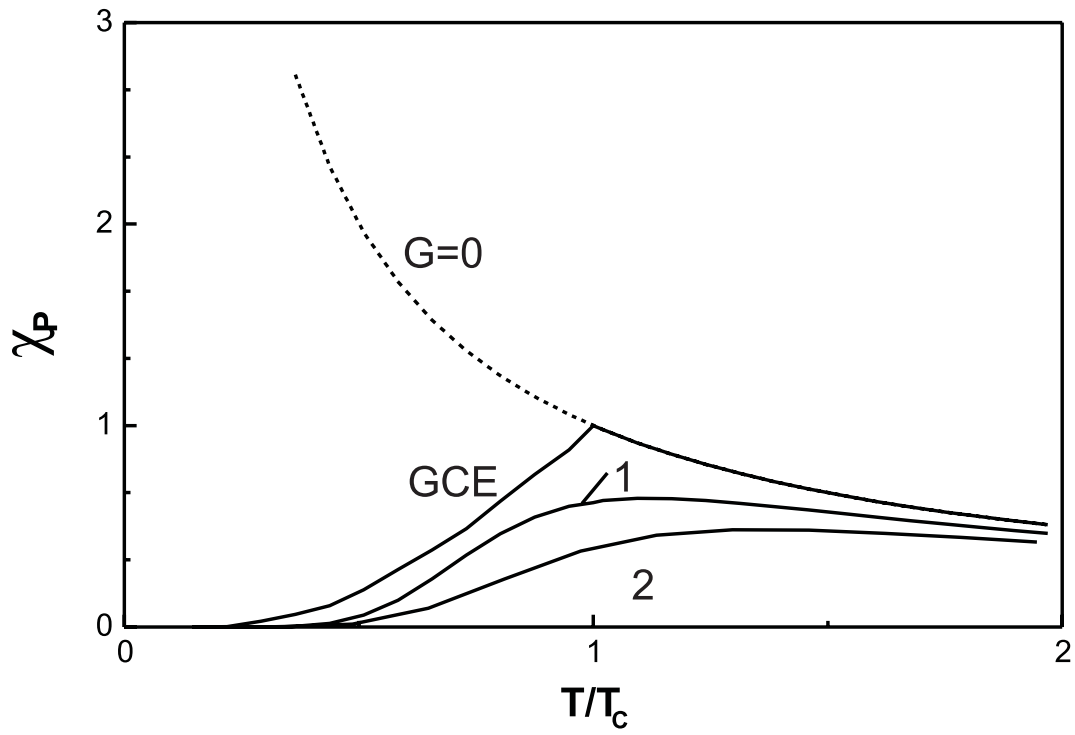


Figure 12: Grand canonical and canonical paramagnetic susceptibilities (in units $\chi_P(G = 0, T = T_c)$) v.s. T/T_c . Curves 1,2 represent the results of canonical calculations of $\chi_P(G > 0)$ for the shell with $M = 11, N_{sh} = 10$ (curve 1) and for the shell with $M = 5, N_{sh} = 5$ (curve 2).